Systematic analysis of strange single heavy baryons Ξ_c and Ξ_b*

Zhen-Yu Li (李振宇)[1†] Guo-Liang Yu (于国梁)[2‡] Zhi-Gang Wang (王志刚)[2§] Jian-Zhong Gu (顾建中)[3]
Jie Lu (卢杰)[2] Hong-Tao Shen (沈洪涛)[4]

[1]School of Physics and Electronic Science, Guizhou Education University, Guiyang 550018, China
[2]Department of Mathematics and Physics, North China Electric Power University, Baoding 071003, China
[3]China Institute of Atomic Energy, Beijing 102413, China
[4]Guangxi Key Laboratory of Nuclear Physics and Technology, Guangxi Normal University, Guilin 541006, China

Abstract: Motivated by the experimental progress in the study of heavy baryons, we investigate the mass spectra of strange single heavy baryons in the λ-mode, using the relativistic quark model and the infinitesimally shifted Gaussian basis function method. We show that experimental results are well captured using the predicted masses. The root mean square radii and radial probability density distributions of the wave functions are analyzed in detail. Meanwhile, the mass spectra allow us to successfully construct the Regge trajectories in the (J, M^2) plane. We also preliminarily assign quantum numbers to the recently observed baryons, including $\Xi_c(3055)$, $\Xi_c(3080)$, $\Xi_c(2930)$, $\Xi_c(2923)$, $\Xi_c(2939)$, $\Xi_c(2965)$, $\Xi_c(2970)$, $\Xi_c(3123)$, $\Xi_b(6100)$, $\Xi_b(6227)$, $\Xi_b(6327)$, and $\Xi_b(6333)$. Finally, the spectral structure of strange single heavy baryons is discussed. Accordingly, we predict several new baryons that may be observed in forthcoming experiments.

Keywords: single heavy baryons, mass spectra, relativistic quark model

DOI: 10.1088/1674-1137/acd365

I. INTRODUCTION

Recently, many single heavy baryons have been observed in experiments, and the mass spectra of single heavy baryon families have become increasingly abundant [1−29]. Such a wealth of experimental data gives theorists an opportunity to test the validity of current theoretical frameworks. In addition, this is a good time to carry out systematic and precise calculations using theoretical methods, for promoting the consistency between experiments and theories.

The strange single heavy baryon Ξ_Q families including Ξ_c ($\Xi_c^{'}$) [1−14] and Ξ_b ($\Xi_b^{'}$) [16−25], are being established step by step, owing to the cooperative efforts of experimentalists and theorists. So far, more than a dozen Ξ_Q baryons have been recorded in the latest particle data group (PDG) [28], even though the J^P values of some baryons remain undetermined, such as those of $\Xi_c(3055)$, $\Xi_c(3080)$ and $\Xi_c(6227)$. Recently, some other Ξ_Q baryons have been observed in experiments, including $\Xi_c(3123)$ [4], $\Xi_c(2930)$ [12], $\Xi_c(2923)$, $\Xi_c(2939)$, $\Xi_c(2964)$ [13], $\Xi_b(6327)$ and $\Xi_b(6333)$ [25]. Accordingly, many theoretical studies have been performed on these baryons, such as $\Xi_c(3055)$ [30−34], $\Xi_c(3080)$ [34, 35], $\Xi_c(2923)^0$ (including $\Xi_c(2939)^0$ and $\Xi_c(2965)^0$) [36], $\Xi_c(2930)^0$ [37], $\Xi_c(2970)$ [38−41], $\Xi_c(3123)$ [42], $\Xi_b(6227)$ [43−47], $\Xi_b(6100)$ [48, 49], and $\Xi_b(6327)$ ($\Xi_b(6333)$) [50]. For identifying their quantum numbers and for assigning them suitable positions in the mass spectra, it is necessary to systematically investigate their spectroscopies.

In recent decades, heavy baryons have been studied using many theoretical methods, including the quark potential model in the heavy quark-light diquark picture [42,51−54], relativistic quark model [55], harmonic oscillator quark model [36], constituent quark model [56−63], chiral quark model [30, 37, 43, 50], chiral perturbation theory [64−68], relativistic flux tube model[42], Bethe-

Received 15 March 2023; Accepted 6 May 2023; Published online 7 May 2023

* Supported by the National Natural Science Foundation of China (11675265, 12175068), the Continuous Basic Scientific Research Project (WDJC-2019-13), the Leading Innovation Project (LC 192209000701) and the Central Government Guidance Funds for Local Scientific and Technological Development of China (Guike ZY22096024)

† E-mail: zhenyvli@163.com
‡ E-mail: yuguoliang2011@163.com
§ E-mail: zgwang@aliyun.com

Salpeter formalism [69], effective Lagrangian approach [44], $^3P_0$ decay model [70−77], lattice quantum chromodynamics (QCD) [78−81], bound state picture [82], light cone QCD sum rules [83−92], and QCD sum rules [93−102].

In particular, it is worth mentioning that Ebert *et al.* [51, 52] put forward a heavy quark-light diquark picture in the framework of a QCD-motivated relativistic quark model, in which an initial three-body problem was reduced to a two-step two-body problem. They systematically studied the spectroscopy and Regge trajectories of heavy baryons and successfully predicted new single heavy baryons. Because the excited states in the heavy quark-light diquark picture are very similar to those of the λ-mode in a three-quark system [60], it would be interesting to investigate the λ-mode in the three-quark system systematically and study the differences between the mass spectra of this mode and the heavy quark-light diquark picture.

In the 1980s, Godfrey and Isgur developed a relativistic quark model, using which they studied the mass spectra of mesons [103]. Then, Capstick and Isgur extended the model to baryons [55]. In the relativistic quark model, the Hamiltonian contains almost all of the interactions between two quarks, which is expected to give accurate calculations for heavy baryon spectra.

The Gaussian expansion method (GEM) and the infinitesimally-shifted Gaussian (ISG) basis functions [104] have been successfully applied to few-body systems in nuclear physics. The ISG method is advantageous for improving the computational accuracy and efficiency associated with the calculations of few-body systems. Recently, they were introduced in the study of heavy baryons [60−62], tetraquarks [105−107] and pentaquarks [108].

Inspired by the above discussion, we combined the relativistic quark model with the ISG method, for investigating the strange single heavy baryon spectra of a three-quark system. For the excited states, we only focused on the λ-mode and compared the results with those of the heavy quark-light diquark picture and some relevant experimental data. The present work is a preliminary attempt to systematically investigate strange single heavy baryon spectra; the method is promising for studying other multiquark systems, including the exotic ones [109−113].

The remainder of this paper is organized as follows. In Sec. II, we briefly describe the methods used in our theoretical calculations, mainly including the relativistic quark model and the GEM(ISG) method. In Sec. III, we present the root mean square radii and the mass spectra of the Ξ_Q baryons, analyze the radial probability distributions, and construct the Regge trajectories. Based on these, we analyze in detail the baryons of recent interest. Finally, the mass spectral structures are demonstrated. Sec. IV lists our conclusions.

II. PHENOMENOLOGICAL METHODS USED IN THIS WORK

A. Relativistic quark model and Jacobi coordinates

The relativistic quark model is based on the hypothesis that baryons may be approximately described in terms of center-of-mass (CM) frame valence-quark configurations, the dynamics of which are governed by a Hamiltonian with a one-gluon exchange dominant component at short distances and with a confinement implemented by a flavor-independent Lorentz-scalar interaction [55]. For a three-quark system, the Hamiltonian reads

$$H = H_0 + V, \tag{1}$$

$$H_0 = \sum_{i=1}^{3}(p_i^2+m_i^2)^{1/2}, \tag{2}$$

$$V = \sum_{i<j}(\tilde{H}_{ij}^{\rm conf}+\tilde{H}_{ij}^{\rm so}+\tilde{H}_{ij}^{\rm hyp}), \tag{3}$$

where $\tilde{H}_{ij}^{\rm conf}$, $\tilde{H}_{ij}^{\rm so}$, and $\tilde{H}_{ij}^{\rm hyp}$ are the confinement, spin-orbit, and hyperfine interactions, respectively. The confinement item includes one-gluon exchange potentials and the linear confined potentials. Due to the relativistic effect, the interactions should be modified with CM momentum-dependent factors. It is worth noting that the forms of the interactions in this paper have been rearranged for ease of use [105, 114]. The interactions were decomposed as follows:

$$\tilde{H}_{ij}^{\rm conf} = G'_{ij}(r)+\tilde{S}_{ij}(r), \tag{4}$$

$$\tilde{H}_{ij}^{\rm so} = \tilde{H}_{ij}^{{\rm so}(v)}+\tilde{H}_{ij}^{{\rm so}(s)}, \tag{5}$$

$$\tilde{H}_{ij}^{\rm hyp} = \tilde{H}_{ij}^{\rm tensor}+\tilde{H}_{ij}^{c}, \tag{6}$$

with

$$\tilde{H}_{ij}^{{\rm so}(v)} = \frac{\mathbf{S}_i\cdot\mathbf{L}_{ij}}{2m_i^2 r_{ij}}\frac{\partial\tilde{G}_{ii}^{{\rm so}(v)}}{\partial r_{ij}}+\frac{\mathbf{S}_j\cdot\mathbf{L}_{ij}}{2m_j^2 r_{ij}}\frac{\partial\tilde{G}_{jj}^{{\rm so}(v)}}{\partial r_{ij}}+\frac{(\mathbf{S}_i+\mathbf{S}_j)\cdot\mathbf{L}_{ij}}{m_i m_j r_{ij}}\frac{\partial\tilde{G}_{ij}^{{\rm so}(v)}}{\partial r_{ij}}, \tag{7}$$

$$\tilde{H}_{ij}^{{\rm so}(s)} = -\frac{\mathbf{S}_i\cdot\mathbf{L}_{ij}}{2m_i^2 r_{ij}}\frac{\partial\tilde{S}_{ii}^{{\rm so}(s)}}{\partial r_{ij}}-\frac{\mathbf{S}_j\cdot\mathbf{L}_{ij}}{2m_j^2 r_{ij}}\frac{\partial\tilde{S}_{jj}^{{\rm so}(s)}}{\partial r_{ij}}, \tag{8}$$

$$\tilde{H}_{ij}^{\rm tensor} = -\frac{\mathbf{S}_i\cdot\mathbf{r}_{ij}\mathbf{S}_j\cdot\mathbf{r}_{ij}/r_{ij}^2 - \frac{1}{3}\mathbf{S}_i\cdot\mathbf{S}_j}{m_i m_j}\times\left(\frac{\partial^2}{\partial r_{ij}^2} - \frac{1}{r_{ij}}\frac{\partial}{\partial r_{ij}}\right)\tilde{G}_{ij}^t, \tag{9}$$

$$\tilde{H}_{ij}^c = \frac{2\mathbf{S}_i\cdot\mathbf{S}_j}{3m_i m_j}\nabla^2\tilde{G}_{ij}^c. \tag{10}$$

The modified terms in Eqs. (4), (7), (8), (9), and (10) are

$$G'_{ij} = \left(1+\frac{p_{ij}^2}{E_iE_j}\right)^{\frac{1}{2}}\tilde{G}_{ij}(r_{ij})\left(1+\frac{p_{ij}^2}{E_iE_j}\right)^{\frac{1}{2}}, \tag{11}$$

$$\tilde{G}_{ij}^{{\rm so}(v)} = \left(\frac{m_im_j}{E_iE_j}\right)^{\frac{1}{2}+\epsilon_{{\rm so}(v)}}\tilde{G}_{ij}(r_{ij})\left(\frac{m_im_j}{E_iE_j}\right)^{\frac{1}{2}+\epsilon_{{\rm so}(v)}}, \tag{12}$$

$$\tilde{S}_{ii}^{{\rm so}(s)} = \left(\frac{m_im_i}{E_iE_i}\right)^{\frac{1}{2}+\epsilon_{{\rm so}(s)}}\tilde{S}_{ij}(r_{ij})\left(\frac{m_im_i}{E_iE_i}\right)^{\frac{1}{2}+\epsilon_{{\rm so}(s)}}, \tag{13}$$

$$\tilde{G}_{ij}^{t} = \left(\frac{m_im_j}{E_iE_j}\right)^{\frac{1}{2}+\epsilon_t}\tilde{G}_{ij}(r_{ij})\left(\frac{m_im_j}{E_iE_j}\right)^{\frac{1}{2}+\epsilon_t}, \tag{14}$$

$$\tilde{G}_{ij}^{c} = \left(\frac{m_im_j}{E_iE_j}\right)^{\frac{1}{2}+\epsilon_c}\tilde{G}_{ij}(r_{ij})\left(\frac{m_im_j}{E_iE_j}\right)^{\frac{1}{2}+\epsilon_c}, \tag{15}$$

where $E_i = \sqrt{m_i^2+p_{ij}^2}$ is the relativistic kinetic energy, and p_{ij} is the momentum magnitude of either of the quarks in the CM frame of the ij quark subsystem [105].

$\tilde{G}_{ij}(r_{ij})$ and $\tilde{S}_{ij}(r_{ij})$ are obtained using the smearing transformations of the one-gluon exchange potential $G(r) = -\frac{4\alpha_s(r)}{3r}$ and linear confinement potential $S(r) = br+c$, respectively,

$$\tilde{G}_{ij}(r_{ij}) = \mathbf{F}_i\cdot\mathbf{F}_j\sum_{k=1}^{3}\frac{2\alpha_k}{\sqrt{\pi}r_{ij}}\int_0^{\tau_{kij}r_{ij}}{\rm e}^{-x^2}{\rm d}x, \tag{16}$$

$$\tilde{S}_{ij}(r_{ij}) = -\frac{3}{4}\mathbf{F}_i\cdot\mathbf{F}_j\left\{br_{ij}\left[\frac{{\rm e}^{-\sigma_{ij}^2r_{ij}^2}}{\sqrt{\pi}\sigma_{ij}r_{ij}} + \left(1+\frac{1}{2\sigma_{ij}^2r_{ij}^2}\right)\frac{2}{\sqrt{\pi}}\int_0^{\sigma_{ij}r_{ij}}{\rm e}^{-x^2}{\rm d}x\right]+c\right\}, \tag{17}$$

with

$$\tau_{kij} = \frac{1}{\sqrt{\frac{1}{\sigma_{ij}^2}+\frac{1}{\gamma_k^2}}}, \tag{18}$$

$$\sigma_{ij} = \sqrt{s^2\left(\frac{2m_im_j}{m_i+m_j}\right)^2+\sigma_0^2\left(\frac{1}{2}\left(\frac{4m_im_j}{(m_i+m_j)^2}\right)^4+\frac{1}{2}\right)}. \tag{19}$$

Here, α_k and γ_k are constants. $\mathbf{F}_i\cdot\mathbf{F}_j$ stands for the inner product of the color matrices of quarks i and j. $\mathbf{F}$ includes 8 components (the so-called Gell-mann matrices), which can be written as

$$F_n = \begin{cases} \dfrac{\hat{\lambda}_n}{2}, & \text{for quarks,} \\ -\dfrac{\hat{\lambda}_n^*}{2}, & \text{for antiquarks,} \end{cases} \tag{20}$$

with $n = 1,\cdots,8$. All of the parameters in these formulas were taken from Table 2 of Ref. [103], except that b and c were revised to 0.14 GeV^2 and –0.198 GeV, respectively. Using the revised b and c values, and setting the values of the other parameters as in Ref. [103], we can reproduce most of the experimental values nicely for single heavy baryons, such as $\Lambda_{c,b}$, $\Sigma_{c,b}$, $\Omega_{c,b}$ (see Ref. [115]) and $\Xi_{c,b}$ (see Tables 1–2 and 4–5 in the appendix of this article).

To represent the internal motion of quarks in a few-body system, one commonly introduces the Jacobi coordinates. As shown in Fig. 1, there are overall three channels of the Jacobi coordinates for the three-body system. The corresponding Jacobi coordinates are defined as

$$\boldsymbol{\rho}_i = \mathbf{r}_j - \mathbf{r}_k, \tag{21}$$

$$\boldsymbol{\lambda}_i = \mathbf{r}_i - \frac{m_j\mathbf{r}_j+m_k\mathbf{r}_k}{m_j+m_k}, \tag{22}$$

where $i, j, k = 1, 2, 3$ (or replace their positions in turn). $\mathbf{r}_i$

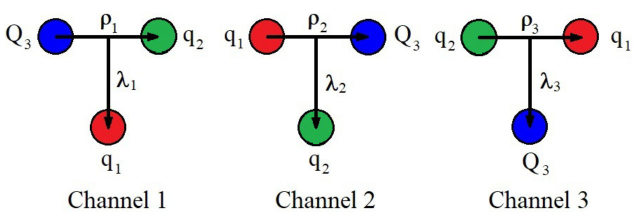

Fig. 1. (color online) Jacobi coordinates for the three-quark system. We denote the heavy quark as the third one in the case of single heavy baryons.

and m_i denote the position vector and the mass of the ith quark, respectively.

We perform our calculations based on channel 3. In this case, the third quark is just the heavy quark, which is consistent with the heavy quark limit [116, 117]. Further, $\mathbf{l}_{\rho 3}$(denoted succinctly as $\mathbf{l}_\rho$) is clearly defined as the orbital angular momentum between the light quarks, and $\mathbf{l}_{\lambda 3}$(denoted succinctly as $\mathbf{l}_\lambda$) represents the one between the heavy quark and the light-quark pair.

B. The heavy quark limit and wave function

In the heavy quark limit, the heavy quark within the heavy baryon system is decoupled from the two light quarks. With the requirement of the flavor $SU(3)$ subgroups for the light quarks, the baryons belong to either a sextet (6_F) of flavor-symmetric states $\Xi_Q^{'}$ or an antitriplet ($\bar{3}_F$) of flavor antisymmetric states Ξ_Q. The flavor wave functions of strange single heavy baryons are

$$\begin{aligned}\Xi_Q^{'} &= \frac{1}{\sqrt{2}}(qq_s+q_sq)Q,\\ \Xi_Q &= \frac{1}{\sqrt{2}}(qq_s-q_sq)Q. \end{aligned}\tag{23}$$

Here q denotes an up or down quark, and Q is a charm or bottom quark, while q_s is a strange quark. For a quantum state with specified angular momenta in this work, the spatial wave function is combined with the spin function, as follows:

$$\begin{aligned}&|l_\rho\ l_\lambda\ L\ s\ j\ J\ M_J\rangle\\ &=\sum_{m_{s_3}=-1/2}^{1/2}\sum_{m_j=-j}^{j}\sum_{M_L=-L}^{L}\sum_{m_s=-s}^{s}\sum_{m_{s_1}=-1/2}^{1/2}\sum_{m_{s_2}=-1/2}^{1/2}\sum_{m_\rho=-l_\rho}^{l_\rho}\sum_{m_\lambda=-l_\lambda}^{l_\lambda}\\ &\quad\times\langle j\ m_j\ s_3\ m_{s_3}|j\ s_3\ J\ M_J\rangle\times\langle L\ M_L\ s\ m_s|L\ s\ j\ m_j\rangle\\ &\quad\times\langle s_1\ m_{s_1}\ s_2\ m_{s_2}|s_1\ s_2\ s\ m_s\rangle\times\langle l_\rho\ m_\rho l_\lambda\ m_\lambda|l_\rho\ l_\lambda\ L\ M_L\rangle\\ &\quad\times|l_\rho\ m_\rho\rangle\otimes|l_\lambda\ m_\lambda\rangle\otimes|s_1\ m_{s_1}\rangle\otimes|s_2\ m_{s_2}\rangle\otimes|s_3\ m_{s_3}\rangle, \end{aligned}\tag{24}$$

with $\mathbf{L}=\mathbf{l}_\rho+\mathbf{l}_\lambda$, $\mathbf{s}=\mathbf{s}_1+\mathbf{s}_2$, $\mathbf{j}=\mathbf{L}+\mathbf{s}$, and $\mathbf{J}=\mathbf{j}+\mathbf{s}_3$. l_ρ, l_λ, L, s, j, J, and M_J are the quantum numbers that characterize a given quantum state in theory. This scheme $|l_\rho\ l_\lambda\ L\ s\ j\ J\ M_J\rangle$ (j-s coupling) is also commonly used for analyzing the strong decay of heavy baryons [74].

C. GEM and ISG

In calculations, the spatial wave function $|l_\rho\ m_\rho\rangle\otimes|l_\lambda\ m_\lambda\rangle$ in formula (24) should be expanded in terms of basis functions. Naturally, one of the candidates is the simple harmonic oscillator (SHO) basis, owing to its good orthogonality. However, the completeness of the SHO is not rigorous in calculations because a truncated set has to be used [55, 103]. Compared with the SHO basis functions, the advantage of the Gaussian basis functions is that they can form an approximately complete set in a finite coordinate space. This is known as the GEM [104].

Following formula (24), the spatial wave function is expanded in terms of a set of Gaussian basis functions,

$$|l_\rho m_\rho\rangle\otimes|l_\lambda m_\lambda\rangle=\sum_{n_\rho=1}^{n_{\max}}\sum_{n_\lambda=1}^{n_{\max}}c_{n_\rho n_\lambda}|n_\rho l_\rho m_\rho\rangle^G\otimes|n_\lambda l_\lambda m_\lambda\rangle^G,\tag{25}$$

where the Gaussian basis function $|nlm\rangle^G$ is commonly written in the position space as

$$\begin{aligned}\phi^G_{nlm}(\mathbf{r})&=\phi^G_{nl}(r)Y_{lm}(\hat{\mathbf{r}}),\\ \phi^G_{nl}(r)&=N_{nl}r^l\mathrm{e}^{-\nu_n r^2},\\ N_{nl}&=\sqrt{\frac{2^{l+2}(2\nu_n)^{l+3/2}}{\sqrt{\pi}(2l+1)!!}},\end{aligned}\tag{26}$$

or in the momentum space as

$$\begin{aligned}\phi'^G_{nlm}(\mathbf{p})&=\phi'^G_{nl}(p)Y_{lm}(\hat{\mathbf{p}}),\\ \phi'^G_{nl}(p)&=N'_{nl}p^l\mathrm{e}^{-\frac{p^2}{4\nu_n}},\\ N'_{nl}&=(-i)^l\sqrt{\frac{2^{l+2}}{\sqrt{\pi}(2\nu_n)^{l+3/2}(2l+1)!!}},\end{aligned}\tag{27}$$

with

$$\begin{aligned}\nu_n&=\frac{1}{r_n^2},\\ r_n&=r_1a^{n-1}\quad(n=1,\ 2,\ ...,\ n_{\max}).\end{aligned}\tag{28}$$

r_1, a, and $n_{\max}$ are the Gaussian size parameters in the geometric progression for numerical calculations, and the final results are stable and independent of these parameters within an approximately complete set in a sufficiently large space.

The Gaussian basis functions are non-orthogonal, which leads to a generalized matrix eigenvalue problem,

$$\sum_{\kappa'=1}^{\kappa_{\max}}[H_{\kappa\kappa'}-E\tilde{N}_{\kappa\kappa'}]c_{\kappa'}=0,\tag{29}$$

with

$$\begin{aligned}\tilde{N}_{\kappa\kappa'}&=\langle\phi^G_{n_\rho l_\rho m_\rho}|\phi^G_{n_{\rho'}l_{\rho'}m_{\rho'}}\rangle\times\langle\phi^G_{n_\lambda l_\lambda m_\lambda}|\phi^G_{n_{\lambda'}l_{\lambda'}m_{\lambda'}}\rangle\\ &=\left(\frac{2\sqrt{\nu_{n_\rho}\nu_{n_{\rho'}}}}{\nu_{n_\rho}+\nu_{n_{\rho'}}}\right)^{l_\rho+3/2}\times\left(\frac{2\sqrt{\nu_{n_\lambda}\nu_{n_{\lambda'}}}}{\nu_{n_\lambda}+\nu_{n_{\lambda'}}}\right)^{l_\lambda+3/2},\end{aligned}\tag{30}$$

where $\kappa=1,\ 2,...,\ \kappa_{\max}$, $\kappa_{\max}=n_{\max}\times n_{\max}$ and $c_\kappa=c_{n_\rho n_\lambda}$.

H and E denote the Hamiltonian and the eigenvalue, respectively.

In the calculation of the Hamiltonian matrix elements of three-body systems, particularly, when complicated interactions are employed, integrations over all of the radial and angular coordinates become laborious even with the Gaussian basis functions. This process can be simplified by introducing the ISG basis functions by

$$\phi^G_{nlm}(\mathbf{r}) = N_{nl} r^l \mathrm{e}^{-\nu_n r^2} Y_{lm}(\hat{\mathbf{r}}) = N_{nl} \lim_{\varepsilon\to 0} \sum_{k=1}^{k_{\max}} C_{lm,k} \mathrm{e}^{-\nu_n(\mathbf{r}-\varepsilon \mathbf{D}_{lm,k})^2}. \tag{31}$$

In formula (31), $Y_{lm}(\hat{\mathbf{r}})$ is replaced by a set of coefficients $C_{lm,k}$ and vectors $\mathbf{D}_{lm,k}$. Thus, the ISG method can effectively avoid the difficulty of spatial angle integration in the calculation of matrix elements. This method is described in detail in literature [104].

III. NUMERICAL RESULTS AND DISCUSSION

A. Numerical stabilities and the λ-mode

The Gaussian size parameters $\{n_{\max}, r_1, r_{n_{\max}}\}$ are related to the scale in question. For example, they are different in Ref. [104] and Ref. [118]. To obtain stable numerical solutions in our calculation, they should be optimized specifically. For the Gaussian functions that constitute a set of non-orthogonal bases in a finite coordinate space, the number of the bases should be in a reasonable range. As shown in Fig. 2, the numerical stability is achieved when the dimension parameter $n_{\max}$ is in the $9\sim 14$ range, with $r_1 = 0.18$ GeV^{-1} and $r_{n_{\max}} = 15$ GeV^{-1}. The value $n_{\max} = 10$ was adopted in this work, using which both the computation efficiency and accuracy were actually satisfied.

$nL(J^P)$ is commonly used to describe baryon states. For angular momentum $L \neq 0$, there exist several $|l_\rho l_\lambda L s j J M_J\rangle$ states satisfying the condition $\mathbf{L} = \mathbf{l}_\rho + \mathbf{l}_\lambda$. They may be divided into the following three modes: (1) the ρ-mode with $l_\rho \neq 0$ and $l_\lambda = 0$; (2) the λ-mode with $l_\rho = 0$ and $l_\lambda \neq 0$; and (3) the λ-ρ mixing mode with $l_\rho \neq 0$ and $l_\lambda \neq 0$.

As an example, the excitation energies of the $1P(\frac{1}{2}^-, \frac{3}{2}^-)_{j=1}$ states of $\bar{3}_F$ as functions of m_Q were investigated, where the dependence of excitation energies on m_Q of the λ-mode was compared with that of the ρ-mode. As shown in Fig. 3, the λ-mode and the ρ-mode became clearly separated when m_Q increased from 1.0 GeV to 5.0 GeV. In the case of 6_F, we reached the same conclusion for $m_Q > 1.5$GeV, as shown in Fig. 4. Besides the p-wave states, the same was observed for higher angular excited states [60]. Thus, we investigated the mass spectrum in the λ-mode.

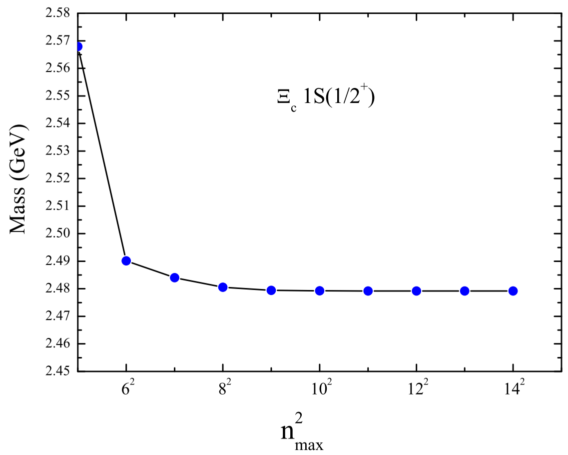

Fig. 2. (color online) Numerical stability of the $\Xi_c 1S(\frac{1}{2}^+)$ mass with respect to the dimension parameter $n_{\max}$.

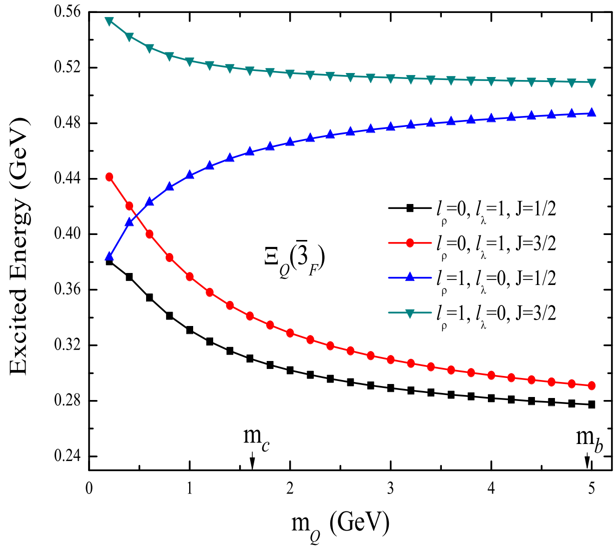

Fig. 3. (color online) Dependence of the excitation energy on m_Q, for different modes of Ξ_Q. The black and red curves represent the λ-mode. The blue and green ones denote the ρ-mode.

B. Mass spectra, root mean square radius and radial probability density distribution

In this subsection, the root mean square radii, radial probability density distributions, and the mass spectra of strange single heavy baryons are presented. For convenience, the relevant experimental data are given together. The detailed results are listed in Tables 1−6 (see the appendix). There are overall four families, namely Ξ_c, $\Xi_c^{'}$, Ξ_b and $\Xi_b^{'}$. The mass spectra of excited states with quantum numbers up to $n = 4$ and $L = 4$ are displayed. Many theoretical studies have been conducted on this subject [35, 44, 52, 56−59, 119, 120]. For reference, the results of some of these studies are included in the following tables.

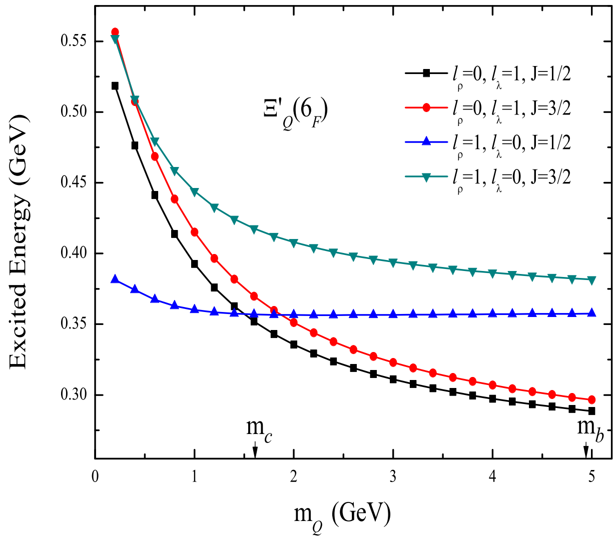

Fig. 4. (color online) Excitation energy versus m_Q, for different modes of Ξ'_Q. Note that the black curve is lower than the blue one with $m_Q > 1.5$GeV, and the red curve is overall lower than the green one ($m_c = 1.628$ GeV and $m_b = 4.977$ GeV were used in this work).

By analyzing these calculated results, some general features of the mass spectra were inferred, as follows. First, Ξ_Q is lower than Ξ'_Q in terms of the energy. This feature has been recognized in light baryons where highly orbitally excited states have an antisymmetric structure that minimizes the energy [121]. Second, the mass splitting of spin-doublet states decreases with increasing L. For example, Table 1 shows that the mass differences for the spin-doublets of $1P$-, $1D$-, $1F$-, and $1G$-wave are 30 MeV, 13 MeV, 5 MeV, and 1 MeV, respectively. Third, for the same L, the mass splitting hardly changes as j increases. For example, Tables 2 and 3 show that the mass differences for $1D$ doublets with $j = 1,2,3$ are 10 MeV, 10 MeV, and 13 MeV, respectively. Finally, the mass difference between two adjacent radial excited states gradually decreases with increasing n, which is clearly different from that given by Ebert *et al.*.

In addition, the calculated root mean square radii and radial probability density distributions carry important information. For a three-quark system, the radial probability densities $\omega(r_\rho)$ and $\omega(r_\lambda)$ can be defined as follows:

$$\omega(r_\rho) = \int |\Psi(\mathbf{r}_\rho,\mathbf{r}_\lambda)|^2 \mathrm{d}\mathbf{r}_\lambda \mathrm{d}\Omega_\rho,$$
$$\omega(r_\lambda) = \int |\Psi(\mathbf{r}_\rho,\mathbf{r}_\lambda)|^2 \mathrm{d}\mathbf{r}_\rho \mathrm{d}\Omega_\lambda, \tag{32}$$

where Ω_ρ and Ω_λ are the solid angles spanned by vectors $\mathbf{r}_\rho$ and $\mathbf{r}_\lambda$, respectively. From Figs. 5–7 and Tables 1-6, one can observe some interesting properties.

(1) For the same n states, when L changes from 1 to 4, their $\langle r_\rho^2\rangle^{1/2}$ values increase slightly. However, their $\langle r_\lambda^2\rangle^{1/2}$ values gradually increase. A similar phenomenon is observed in Figs. 5 and 6, where the radial probability of $r_\rho^2\omega(r_\rho)$ changes slightly with different L values. However, the peak value of $r_\lambda^2\omega(r_\lambda)$ significantly shifts outward with increasing L.

(2) For the same L states, $\langle r_\rho^2\rangle^{1/2}$ and $\langle r_\lambda^2\rangle^{1/2}$ generally increase with increasing n. The peaks of their probability densities in general shift outward, as shown in Fig. 7.

(3) The shapes of the eight black (solid) lines in Fig. 5 are almost the same as those in Fig. 6. The values of $\langle r_\rho^2\rangle^{1/2}$ for the same state are almost the same for the $\Xi_c(\Xi'_c)$ and $\Xi_b(\Xi'_b)$ families. This reflects the fact that the

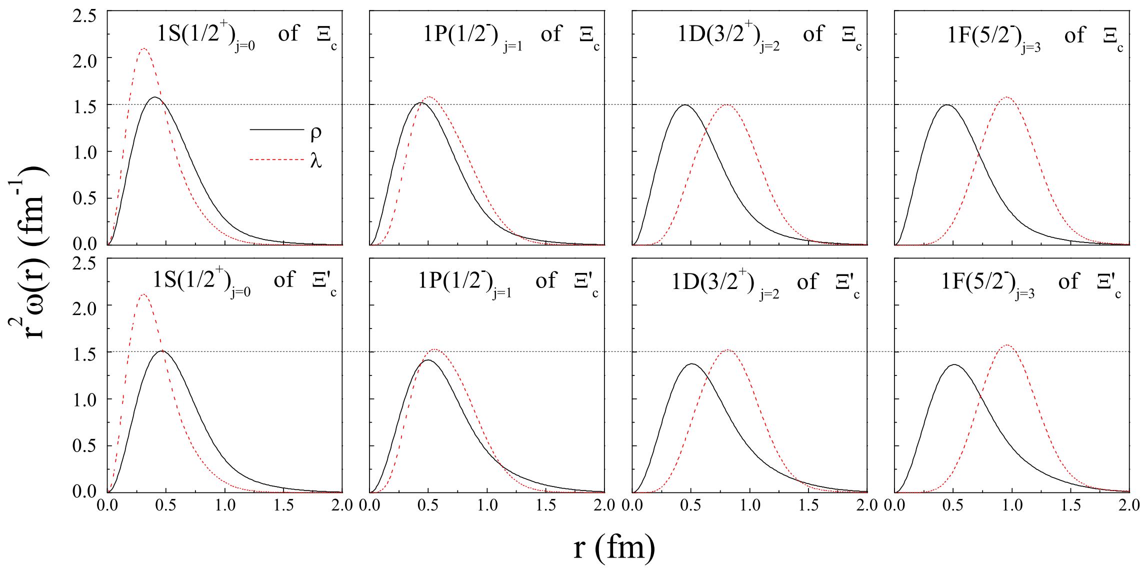

Fig. 5. (color online) Radial probability density distributions for some $1L$ states in the Ξ_c and Ξ'_c families. The solid line denotes the probability density with r_ρ, and the dashed line denotes the one with r_λ.

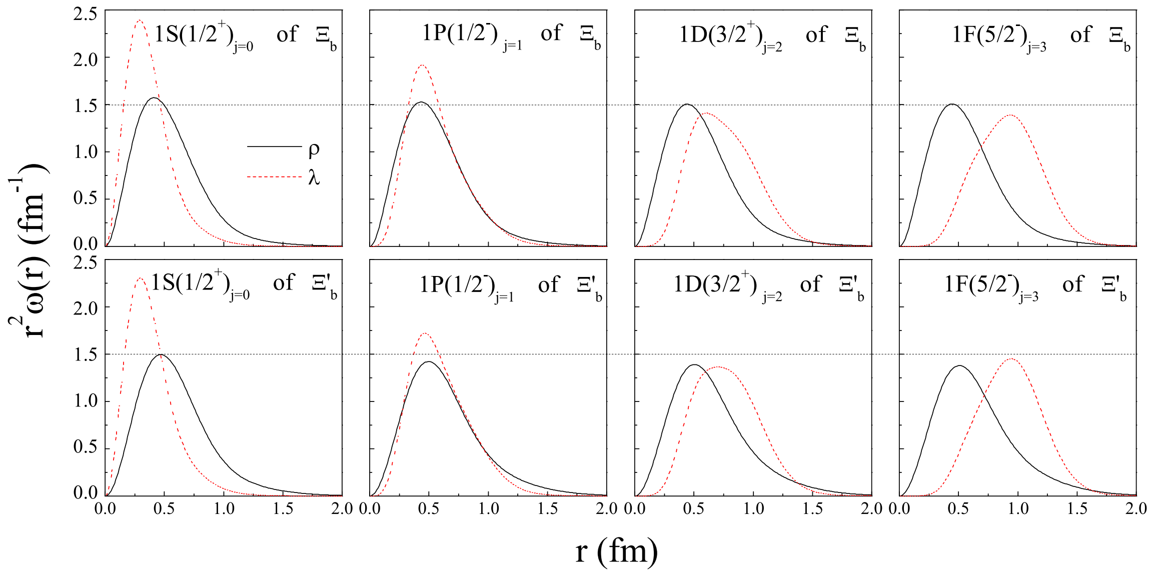

Fig. 6. (color online) Same as for Fig. 5, but for the Ξ_b and $\Xi_b^{\prime}$ families.

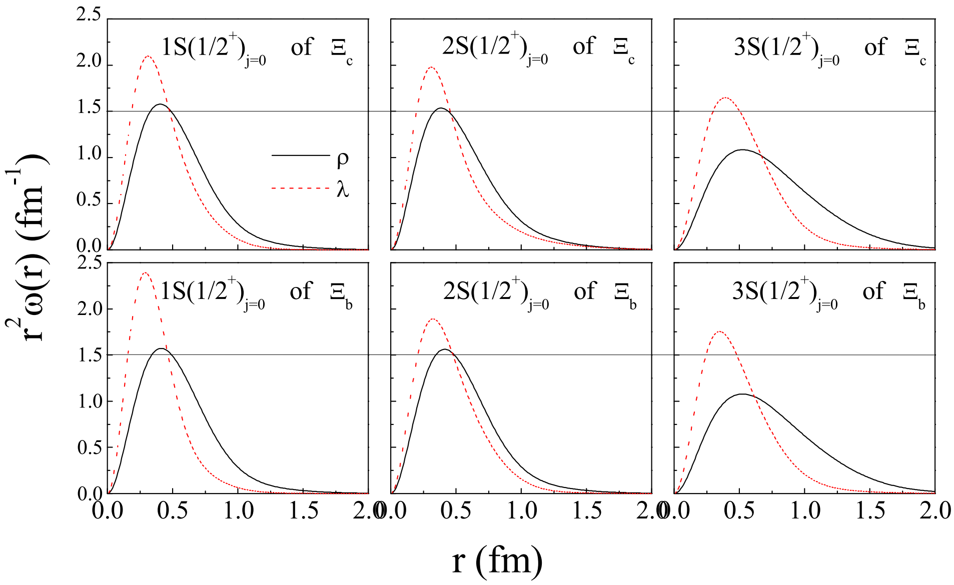

Fig. 7. (color online) Radial probability density distributions for some nS states in the Ξ_c and Ξ_b families.

configurations of the two light quarks in the $\Xi_c(\Xi_c^{\prime})$ and $\Xi_b(\Xi_b^{\prime})$ baryons are similar to each other.

(4) As shown in Tables 1−6, the root mean square radii of those baryons that have been experimentally well established are generally less than 0.8 fm.

As the root mean square radius increases, the radial probability distribution of the wave function becomes more outwardly extended, and baryons become looser. In general, the root mean square radius of a compact baryon is within a threshold, which is helpful for estimating the upper limit of the corresponding mass spectrum and for constraining the number of members in each heavy baryon family.

C. Regge trajectories

Regge trajectories is an effective method for describing hadron mass spectra [122−126]. In 2011, Ebert *et al.* constructed the heavy baryon Regge trajectories for both the (J,M^2) and (n,M^2) planes [52].

In this subsection, we investigate the Regge trajectories in the (J,M^2) plane based on our calculated mass spectra. The states in a baryon family can be classified according to the following parities and angular momenta: (1) natural $P=(-1)^{J+1/2}$ and unnatural $P=(-1)^{J-1/2}$ parities (written in short as NP and UP, respectively) [127]; (2) $J=j+1/2$ and $J=j-1/2$ (written in short as NJ and UJ). Thus, the states in the Ξ_c or Ξ_b family are divided into two groups, and the states in the Ξ_c' or Ξ_b' family are divided into six groups. In this paper, we use the following definition for the (J,M^2) Regge trajectories:

$$M^2 = \alpha J + \beta, \tag{33}$$

where α and β are the slope and intercept. In Figs. 8 and 9, we plot the Regge trajectories in the (J,M^2) plane. The three lines in each figure correspond to the radial quantum numbers n = 1, 2, 3, respectively. The fitted slopes and intercepts of the Regge trajectories are listed in Tables 7 and 8.

Linear trajectories appear clearly in the (J,M^2) plane. All the data points fall on the trajectory lines. This indicates that the Regge trajectory is strongly universal, and our theoretical calculations are reliable. These trajectories are almost parallel but not equidistant, which is an apparent difference between our mass spectra and those in Ref. [52].

In this paper, we do not show the Regge trajectories in the (n,M^2) plane. In fact, linear trajectories in the (n,M^2) plane can not be constructed from our predicted masses. As will be mentioned in subsection III.E, if the observation of heavy baryons in forthcoming experiments touches the 3S sub shell, it will allow to check the (n,M^2) Regge trajectories, which in turn will allow to determine whether a single heavy baryon is a three-quark system or a quark-diquark system.

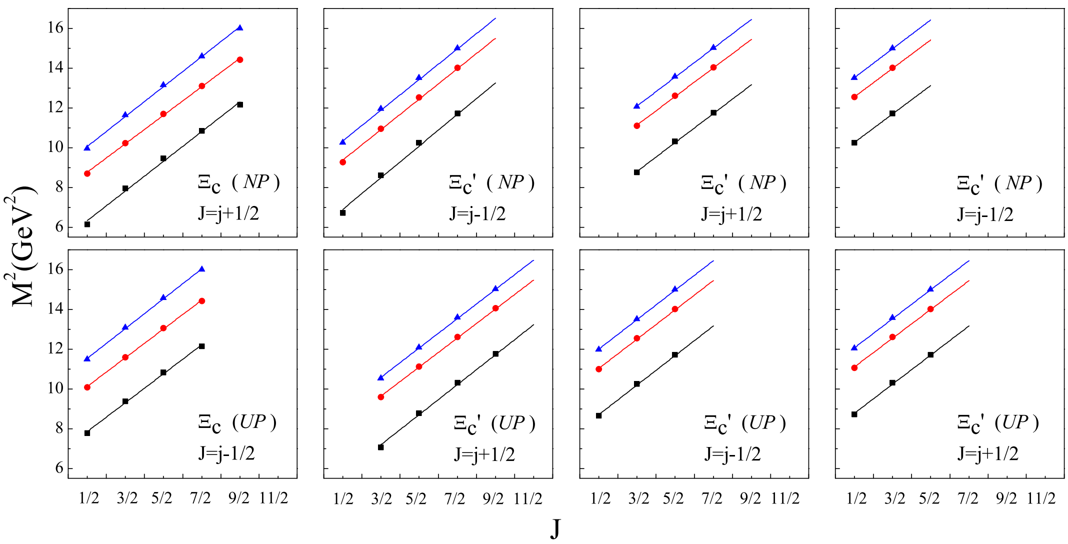

Fig. 8. (color online) (J,M^2) Regge trajectories for the Ξ_c (Ξ_c') families, with M^2 in GeV^2.

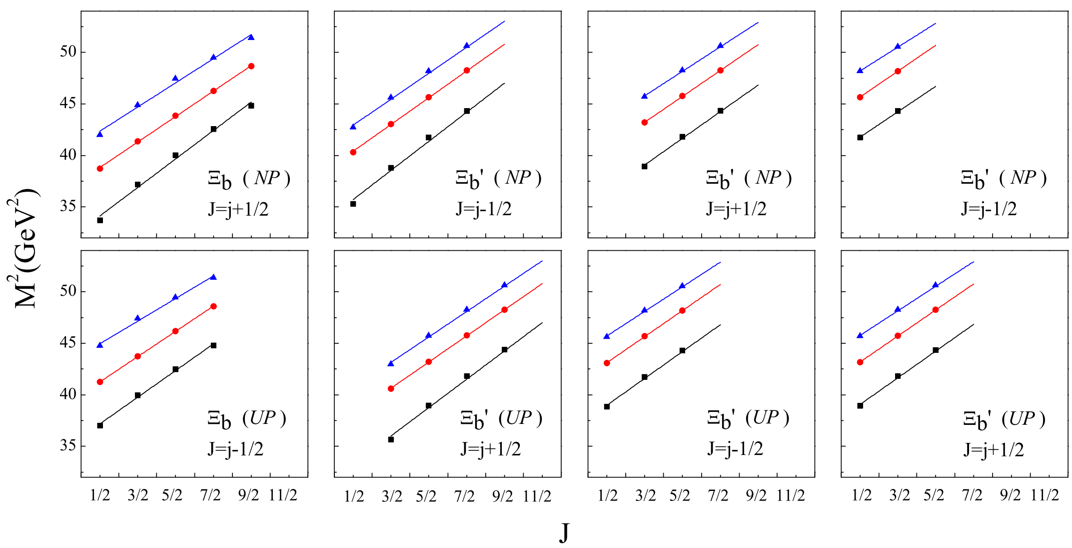

Fig. 9. (color online) (J,M^2) Regge trajectories for the Ξ_b (Ξ_b') families, with M^2 in GeV^2.

D. Preliminary assignment to some observed heavy baryons

For the well determined Ξ_c ($\Xi_c^{'}$) baryons in the PDG, we can assign them to the corresponding positions as follows: Ξ_c^{+} and $\Xi_c^{0} \leftrightarrow \Xi_c 1S(\frac{1}{2}^{+})$, $\Xi_c^{'+,0} \leftrightarrow \Xi_c 1S(\frac{1}{2}^{+})$, $\Xi_c(2645)^{+,0} \leftrightarrow \Xi_c^{'} 1S(\frac{3}{2}^{+})$, and $\Xi_c(2790)^{+,0}$ and $\Xi_c(2815)^{+,0} \leftrightarrow \Xi_c 1P(\frac{1}{2}^{-}, \frac{3}{2}^{-})$, as listed in Tables 1 and 2. The measured masses are well reproduced in our calculations, and the deviation is usually below 14 MeV. In addition, it should be noted that $\Xi_c(2645)$ in the PDG should be labelled with $\Xi_c^{'}(2645)$.

$\Xi_c(2970)$, previously known as $\Xi_c(2980)$, was first observed by Belle in 2006 [29]. The quantum numbers of $\Xi_c(2970)$ were determined as $\frac{1}{2}^{+}$ in the latest PDG. In our calculations, the only candidate was $2S(\frac{1}{2}^{+})$ of Ξ_c, as shown in Table 1. The predicted mass was 15 MeV less than the experimental result. Finally, $\Xi_c(3055)$ and $\Xi_c(3080)$ were observed by BABAR [4] and Belle [10, 15]. As shown in the PDG, their spin and parity values have not yet been elucidated. According to the measured masses, $\Xi_c(3055)$ and $\Xi_c(3080)$ were likely the $1D$ doublet ($\frac{3}{2}^{+}$, $\frac{5}{2}^{+}$) of Ξ_c in Table 1 or the $2S$ doublet ($\frac{1}{2}^{+}$, $\frac{3}{2}^{+}$) of $\Xi_c^{'}$ in Table 2. Considering that the system with a smaller root mean square radius (especially for $\langle r_\lambda^2\rangle^{1/2}$) was more stable, the $2S$ doublet states should be the ideal candidates.

Outside of the PDG data, Belle and the LHCb observed four charm-strange baryons, namely $\Xi_c(2930)$ [12], $\Xi_c(2923)$, $\Xi_c(2939)$, and $\Xi_c(2964)$ [13], whose masses were very close to each other. By the predicted masses in Tables 1 and 2, the above four baryons can be assigned to be the first orbital ($1P$) excitation of $\Xi_c^{'}$. At present, we can not determine their quantum numbers accurately.

$\Xi_c(3123)$ was observed by the BABAR Collaboration [4]. However, it has not yet appeared in the PDG [28]. In our calculations, the predicted masses of $\Xi_c 3S(\frac{1}{2}^{+})$ and $\Xi_c^{'} 2S(\frac{3}{2}^{+})$ were 3155 MeV and 3095 MeV, respectively, relatively closer to the measured value of $\Xi_c(3123)$ than those of other states. Because $\Xi_c^{'} 2S(\frac{3}{2}^{+})$ has been considered as the candidate of $\Xi_c(3080)$, $\Xi_c(3123)$ is likely the $\Xi_c 3S(\frac{1}{2}^{+})$ state. Of course, whether $\Xi_c(3123)$ exists remains to be tested.

The calculated mass spectra of Ξ_b and $\Xi_b^{'}$ families are listed in Tables 4–6 where overall six bottom-strange baryons with determined quantum numbers in the PDG have been assigned to the possible states, such as $\Xi_b^{-,0} \leftrightarrow \Xi_b 1S(\frac{1}{2}^{+})$, $\Xi_b^{'}(5935)^{-} \leftrightarrow \Xi_b^{'} 1S(\frac{1}{2}^{+})$, and $\Xi_b(5945)^{0}$ and $\Xi_b(5955)^{-} \leftrightarrow \Xi_b^{'} 1S(\frac{3}{2}^{+})$.

In 2021, the AMS collaboration determined $\Xi_b(6100)$ with the quantum numbers $J^P = \frac{3}{2}^{-}$ by measuring the typical decay chain of $\Xi_b(6100)^{-} \to \Xi_b^{*0}\pi^{-} \to \Xi_b^{-}\pi^{+}\pi^{-}$ [24]. Very recently, the values of $J^P = \frac{3}{2}^{-}$ of $\Xi_b(6100)$ were written into the PDG data. Table 4 shows that the mass of $\Xi_b(6100)$ is very close to that of the $\Xi_b 1P(\frac{3}{2}^{-})$ state. Therefore, $\Xi_b(6100)$ is most likely the $1P(\frac{3}{2}^{-})$ state of Ξ_b. From Tables 4 and 5, we find that the experimental data can be well reproduced by our theoretical calculations. In addition, it should be pointed out that $\Xi_b(5945)^{0}$ and $\Xi_b(5955)^{-}$ in the PDG ought to be labelled with $\Xi_b^{'}(5945)^{0}$ and $\Xi_b^{'}(5955)^{-}$.

The last two Ξ_b baryons in the PDG, $\Xi_b(6227)^{-}$ and $\Xi_b(6227)^{0}$, were reported by the LHCb Collaboration in 2018 [23]. However, their spin and parity values are still not confirmed. In Tables 4 and 5, there are six states (one $2S$ state of Ξ_b and five $1P$ states of $\Xi_b^{'}$) whose masses range from 6224 MeV to 6243 MeV. Each of them could be considered as a possible assignment to $\Xi_b(6227)$.

In 2021, two bottom-strange baryons $\Xi_b(6327)$ and $\Xi_b(6333)$ were reported by the LHCb Collaboration. Very recently, the LHCb implied in experiment that they should belong to the Ξ_b 1D($\frac{3}{2}^{+}$, $\frac{5}{2}^{+}$) doublet [25]. In Table 4, one can see that the predicted masses of the 1D doublet ($\frac{3}{2}^{+}$, $\frac{5}{2}^{+}$) of Ξ_b indeed match with the experimental data of $\Xi_b(6327)$ and $\Xi_b(6333)$.

E. Shell structure of the mass spectra

The shell structures of the mass spectra are shown in Figs. 10 and 11, where only the states with their root mean square radii less than 1 fm were collected. In these two figures, the well established baryons in the experiment were labeled next to the corresponding states, and for the recently observed baryons, their possible positions were arranged preliminarily according to the discussions in subsection III.D.

From these two figures, we obtain a bird's-eye view of the mass spectra. Firstly, the baryon spectra of Ξ_c ($\Xi_c^{'}$) and Ξ_b ($\Xi_b^{'}$) have almost the same shell structures. Secondly, the baryons with lighter masses were discovered earlier in experiments. Thirdly, there is a serious energy degeneracy in the P, D and F states for the $\Xi_c^{'}$ ($\Xi_b^{'}$) family. In addition, the calculated masses for the $2S$ states of the Ξ_c (Ξ_b) family are very close to those of the $1P$ states of the $\Xi_c^{'}$ ($\Xi_b^{'}$) family. This makes these states hard to be identified in experiments.

Finally, the states that can be possibly observed experimentally can be predicted. For the Ξ_c family, the $1D$ doublets and the $3S(1/2)^{+}$ are likely to be experimentally observed first. With respect to the $\Xi_c^{'}$ family, the $3S$ doublets might be the next ones to be observed. However, the predicted mass range of the $3S$ doublet states overlaps heavily with that of the $1D$ states. As to the Ξ_b family, we find that the $1P(1/2)^{-}$ state should have been discovered earlier in experiments and the predicted mass would be 6084 MeV. The possibly observed states in the

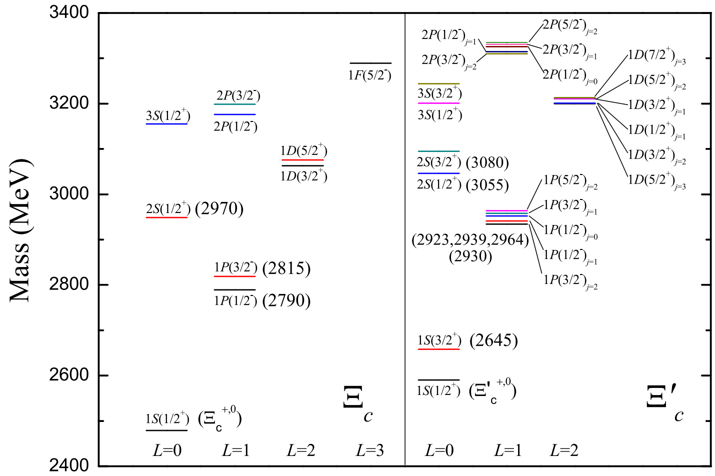

Fig. 10. (color online) Mass spectrum shells of the Ξ_c and $\Xi_c^{'}$ families.

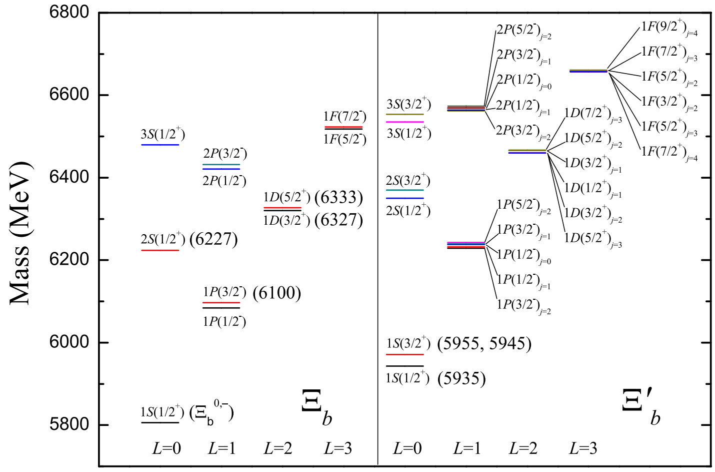

Fig. 11. (color online) Mass spectrum shells of the Ξ_b and $\Xi_b^{'}$ families.

$\Xi_b^{'}$ family should be the $1P$ states where experimental observations will encounter the difficulty of an energy degeneracy.

IV. CONCLUSIONS

Motivated by the experimental developments associated with single heavy baryons, we investigated the strange single heavy baryon spectra in a three-quark system, where the relativistic quark model and the ISG method were employed. Considering that the λ-mode appears lower in terms of the energy for definite states $nL(J^P)$, we only focused on the λ-mode and obtained the mass spectra of the Ξ_c, $\Xi_c^{'}$, Ξ_b, and $\Xi_b^{'}$ families. For the well established baryons, our predicted masses reproduced existing experimental data accurately. We also investigated the root mean square radii and the radial probability density distributions, from which we learned more about the structure of strange single heavy baryons.

Based on the predicted mass spectra, we constructed the Regge trajectories in the (J, M^2) plane. Nevertheless, we could not construct linear trajectories in the (n, M^2) plane, which is an apparent difference between our mass spectra and those in the relativistic quark-diquark picture [52].

For some recently observed baryons, we preliminarily determined their reasonable positions in the mass spectra. Finally, the mass spectral structures of the Ξ_c ($\Xi_c^{'}$) and Ξ_b ($\Xi_b^{'}$) families were presented, from which we obtained a bird's-eye view of the mass spectra and were able to easily foresee the experimental course. Then, we analyzed some states that might be observed in the forthcoming experiments.

ACKNOWLEDGEMENTS

Zhen-yu Li, one of the authors, thanks Wen-chao Dong for his valuable reference, helpful discussion, and kind help in programming. Li is also grateful to Professor Xian-Jian Shi for his encouragement. The authors would like to thank the editors for polishing and typesetting this article.

APPENDIX

Table 1. Root mean square radii (fm) and the mass spectra (MeV) of the Ξ_c family.

$l_\rho l_\lambda L s j$	$nL(J^P)$	$\langle r_\rho^2\rangle^{1/2}$	$\langle r_\lambda^2\rangle^{1/2}$	mass	exp.[28]	[52]	[56]	[57]	[58]
0 0 0 0 0	$1S(\frac{1}{2}^+)$	0.512	0.437	2479	Ξ_c^+ 2467.71(0.23) Ξ_c^0 2470.44(0.28)	2476	2466	2470	2471
	$2S(\frac{1}{2}^+)$	0.645	0.768	2949	$\Xi_c(2970)$?	2959		2940	2964
	$3S(\frac{1}{2}^+)$	0.968	0.607	3155	3123?[4]	3323		3265	3358
	$4S(\frac{1}{2}^+)$	0.690	1.131	3318		3632			3720
0 1 1 0 1	$1P(\frac{1}{2}^-)$	0.542	0.627	2789	2791.9(0.5) 2793.9(0.5)	2792	2773	2793	2796
	$2P(\frac{1}{2}^-)$	0.615	0.948	3176		3179		3140	3191
	$3P(\frac{1}{2}^-)$	1.038	0.763	3390		3500			3541
	$4P(\frac{1}{2}^-)$	0.655	1.285	3492		3785			3879
0 1 1 0 1	$1P(\frac{3}{2}^-)$	0.550	0.654	2819	2816.51(0.25) 2819.79(0.30)	2819	2783	2820	2820
	$2P(\frac{3}{2}^-)$	0.613	0.977	3199		3201		3164	3184
	$3P(\frac{3}{2}^-)$	1.053	0.779	3412		3519			3533
	$4P(\frac{3}{2}^-)$	0.645	1.278	3508		3804			3871
0 2 2 0 2	$1D(\frac{3}{2}^+)$	0.561	0.825	3063		3059	3012	3033	3116
	$2D(\frac{3}{2}^+)$	0.601	1.161	3406		3388			3464
	$3D(\frac{3}{2}^+)$	1.084	0.936	3617		3678			3804
	$4D(\frac{3}{2}^+)$	0.627	1.349	3676		3945			4132
0 2 2 0 2	$1D(\frac{5}{2}^+)$	0.565	0.843	3076		3076	3004	3040	3103
	$2D(\frac{5}{2}^+)$	0.604	1.190	3419		3407			3452
	$3D(\frac{5}{2}^+)$	1.092	0.945	3627		3699			3792
	$4D(\frac{5}{2}^+)$	0.618	1.328	3688		3965			4121
0 3 3 0 3	$1F(\frac{5}{2}^-)$	0.567	0.998	3289		3278			3388
	$2F(\frac{5}{2}^-)$	0.604	1.413	3613		3572			3727
	$3F(\frac{5}{2}^-)$	1.103	1.087	3817		3845			4055
	$4F(\frac{5}{2}^-)$	0.602	1.314	3861		4098			4376
0 3 3 0 3	$1F(\frac{7}{2}^-)$	0.569	1.009	3294		3292			3369
	$2F(\frac{7}{2}^-)$	0.607	1.439	3619		3592			3710
	$3F(\frac{7}{2}^-)$	1.111	1.088	3821		3865			4042
	$4F(\frac{7}{2}^-)$	0.589	1.290	3871		4120			4364
0 4 4 0 4	$1G(\frac{7}{2}^+)$	0.566	1.147	3486		3469	3215		3647
	$2G(\frac{7}{2}^+)$	0.612	1.676	3798		3745			3981
	$3G(\frac{7}{2}^+)$	1.121	1.205	4000					4303
	$4G(\frac{7}{2}^+)$	0.559	1.222	4054					
0 4 4 0 4	$1G(\frac{9}{2}^+)$	0.567	1.154	3487		3483			3627
	$2G(\frac{9}{2}^+)$	0.613	1.692	3799		3763			3960
	$3G(\frac{9}{2}^+)$	1.126	1.208	4001					4285
	$4G(\frac{9}{2}^+)$	0.551	1.202	4064					

Table 2. Root mean square radii (fm) and the mass spectra (MeV) of the Ξ_c' family (Part I).

$l_\rho l_\lambda L s j$	$nL(J^P)$	$\langle r_\rho^2\rangle^{1/2}$	$\langle r_\lambda^2\rangle^{1/2}$	mass	exp.[28]	[52]	[56]	[57]	[58]
0 0 0 1 1	$1S(\frac{1}{2}^+)$	0.590	0.431	2590	$\Xi_c'^+$ 2578.2(0.5) $\Xi_c'^0$ 2578.7(0.5)	2579	2594	2579	
	$2S(\frac{1}{2}^+)$	0.821	0.705	3046	$\Xi_c(3055)$?	2983		2977	
	$3S(\frac{1}{2}^+)$	0.918	0.671	3201		3377		3215	
	$4S(\frac{1}{2}^+)$	0.897	1.053	3425		3695			
0 0 0 1 1	$1S(\frac{3}{2}^+)$	0.611	0.476	2658	2645.10(0.30) 2646.16(0.25)	2654	2649	2649	2648
	$2S(\frac{3}{2}^+)$	0.801	0.763	3095	$\Xi_c(3080)$?	3026		3007	3080
	$3S(\frac{3}{2}^+)$	0.968	0.676	3244		3396		3236	3424
	$4S(\frac{3}{2}^+)$	0.850	1.095	3456		3709			3763
0 1 1 1 0	$1P(\frac{1}{2}^-)$	0.649	0.671	2952		2936		2900	
	$2P(\frac{1}{2}^-)$	0.762	0.978	3326		3313		3144	
	$3P(\frac{1}{2}^-)$	1.055	0.811	3469		3630			
	$4P(\frac{1}{2}^-)$	0.783	1.245	3636		3912			
0 1 1 1 1	$1P(\frac{1}{2}^-)$	0.644	0.659	2941		2854	2855	2839	2832
	$2P(\frac{1}{2}^-)$	0.763	0.962	3315		3267		3094	3195
	$3P(\frac{1}{2}^-)$	1.048	0.804	3460		3598			3545
	$4P(\frac{1}{2}^-)$	0.788	1.248	3628		3887			3883
0 1 1 1 1	$1P(\frac{3}{2}^-)$	0.651	0.677	2958		2935	2866	2932	
	$2P(\frac{3}{2}^-)$	0.761	0.985	3331		3311		3165	
	$3P(\frac{3}{2}^-)$	1.059	0.814	3473		3628			
	$4P(\frac{3}{2}^-)$	0.780	1.243	3640		3911			
0 1 1 1 2	$1P(\frac{3}{2}^-)$	0.642	0.653	2934		2912		2921	2824
	$2P(\frac{3}{2}^-)$	0.764	0.955	3310		3293		3172	3188
	$3P(\frac{3}{2}^-)$	1.043	0.801	3456		3613			3537
	$4P(\frac{3}{2}^-)$	0.791	1.249	3624		3898			3875
0 1 1 1 2	$1P(\frac{5}{2}^-)$	0.652	0.682	2964		2929	2895	2927	2814
	$2P(\frac{5}{2}^-)$	0.761	0.993	3335		3303		3170	3177
	$3P(\frac{5}{2}^-)$	1.062	0.817	3477		3619			3527
	$4P(\frac{5}{2}^-)$	0.778	1.241	3644		3902			3865
0 2 2 1 1	$1D(\frac{1}{2}^+)$	0.668	0.851	3201		3163		3075	3131
	$2D(\frac{1}{2}^+)$	0.744	1.195	3541		3505			3478
	$3D(\frac{1}{2}^+)$	1.104	0.955	3676					3817
	$4D(\frac{1}{2}^+)$	0.738	1.303	3816					4144
0 2 2 1 1	$1D(\frac{3}{2}^+)$	0.671	0.865	3211		3167		3081	
	$2D(\frac{3}{2}^+)$	0.745	1.219	3550		3506			
	$3D(\frac{3}{2}^+)$	1.111	0.963	3684					
	$4D(\frac{3}{2}^+)$	0.734	1.285	3827					

Table 3. Root mean square radii (fm) and the mass spectra (MeV) of the Ξ_c' family (Part II).

$l_\rho l_\lambda L s j$	$nL(J^P)$	$\langle r_\rho^2\rangle^{1/2}$	$\langle r_\lambda^2\rangle^{1/2}$	mass	[52]	[56]	[57]	[58]
0 2 2 1 2	$1D(\frac{3}{2}^+)$	0.668	0.851	3201	3160		3089	3121
	$2D(\frac{3}{2}^+)$	0.744	1.195	3541	3497			3469
	$3D(\frac{3}{2}^+)$	1.104	0.955	3676				3308
	$4D(\frac{3}{2}^+)$	0.738	1.303	3816				4136
0 2 2 1 2	$1D(\frac{5}{2}^+)$	0.671	0.865	3211	3166	3080	3077	
	$2D(\frac{5}{2}^+)$	0.745	1.219	3551	3504			
	$3D(\frac{5}{2}^+)$	1.111	0.963	3685				
	$4D(\frac{5}{2}^+)$	0.734	1.285	3828				
0 2 2 1 3	$1D(\frac{5}{2}^+)$	0.667	0.850	3200	3153		3091	3108
	$2D(\frac{5}{2}^+)$	0.744	1.193	3540	3493			3457
	$3D(\frac{5}{2}^+)$	1.104	0.954	3676				3796
	$4D(\frac{5}{2}^+)$	0.738	1.304	3815				4125
0 2 2 1 3	$1D(\frac{7}{2}^+)$	0.672	0.868	3213	3147	3094	3078	3092
	$2D(\frac{7}{2}^+)$	0.746	1.224	3552	3486			3442
	$3D(\frac{7}{2}^+)$	1.112	0.965	3686				3782
	$4D(\frac{7}{2}^+)$	0.733	1.281	3829				4112
0 3 3 1 2	$1F(\frac{3}{2}^-)$	0.676	1.022	3424	3418			3408
	$2F(\frac{3}{2}^-)$	0.742	1.454	3744				3745
	$3F(\frac{3}{2}^-)$	1.136	1.096	3872				4069
	$4F(\frac{3}{2}^-)$	0.699	1.262	4010				4388
0 3 3 1 2	$1F(\frac{5}{2}^-)$	0.678	1.031	3428	3408			
	$2F(\frac{5}{2}^-)$	0.744	1.474	3748				
	$3F(\frac{5}{2}^-)$	1.140	1.101	3876				
	$4F(\frac{5}{2}^-)$	0.698	1.243	4020				
0 3 3 1 3	$1F(\frac{5}{2}^-)$	0.676	1.022	3424	3394	2989		3393
	$2F(\frac{5}{2}^-)$	0.742	1.454	3744				3732
	$3F(\frac{5}{2}^-)$	1.136	1.096	3872				4059
	$4F(\frac{5}{2}^-)$	0.699	1.263	4009				4379
0 3 3 1 3	$1F(\frac{7}{2}^-)$	0.678	1.031	3428	3393			
	$2F(\frac{7}{2}^-)$	0.744	1.475	3748				
	$3F(\frac{7}{2}^-)$	1.140	1.101	3876				
	$4F(\frac{7}{2}^-)$	0.698	1.242	4021				
0 3 3 1 4	$1F(\frac{7}{2}^-)$	0.676	1.021	3423	3373			3375
	$2F(\frac{7}{2}^-)$	0.742	1.453	3744				3715
	$3F(\frac{7}{2}^-)$	1.136	1.095	3872				4046
	$4F(\frac{7}{2}^-)$	0.699	1.264	4009				4368
0 3 3 1 4	$1F(\frac{9}{2}^-)$	0.678	1.032	3428	3357			3358
	$2F(\frac{9}{2}^-)$	0.744	1.476	3749				3695
	$3F(\frac{9}{2}^-)$	1.140	1.102	3876				4030
	$4F(\frac{9}{2}^-)$	0.698	1.241	4021				4354

Table 4. Root mean square radii (fm) and the mass spectra (MeV) of the Ξ_b family.

$l_\rho l_\lambda L s j$	$nL(J^P)$	$\langle r_\rho^2\rangle^{1/2}$	$\langle r_\lambda^2\rangle^{1/2}$	mass	exp.[28]	[52]	[56]	[59]
0 0 0 0 0	$1S(\frac{1}{2}^+)$	0.518	0.400	5806	Ξ_c^+ 2467.71(0.23) Ξ_c^0 2470.44(0.28)	5803	5806	5796
	$2S(\frac{1}{2}^+)$	0.607	0.705	6224		6266		6208
	$3S(\frac{1}{2}^+)$	0.990	0.549	6480		6601		6533
	$4S(\frac{1}{2}^+)$	0.672	1.066	6568		6913		6825
0 1 1 0 1	$1P(\frac{1}{2}^-)$	0.539	0.571	6084		6120	6090	6137
	$2P(\frac{1}{2}^-)$	0.586	0.844	6421		6496		6341
	$3P(\frac{1}{2}^-)$	1.034	0.713	6690		6805		6520
	$4P(\frac{1}{2}^-)$	0.673	1.281	6732		7068		6679
0 1 1 0 1	$1P(\frac{3}{2}^-)$	0.543	0.583	6097	6100.3(0.6)	6130	6093	6135
	$2P(\frac{3}{2}^-)$	0.585	0.853	6432		6502		6339
	$3P(\frac{3}{2}^-)$	1.043	0.719	6700		6810		6519
	$4P(\frac{3}{2}^-)$	0.668	1.293	6739		7073		6678
0 2 2 0 2	$1D(\frac{3}{2}^+)$	0.551	0.743	6320		6366	6311	6243
	$2D(\frac{3}{2}^+)$	0.568	0.962	6613		6690		6438
	$3D(\frac{3}{2}^+)$	0.990	1.040	6883		6966		6610
	$4D(\frac{3}{2}^+)$	0.778	1.359	6890		7208		6762
0 2 2 0 2	$1D(\frac{5}{2}^+)$	0.553	0.751	6327		6373	6300	6240
	$2D(\frac{5}{2}^+)$	0.568	0.967	6621		6696		6436
	$3D(\frac{5}{2}^+)$	0.948	1.124	6888		6970		6608
	$4D(\frac{5}{2}^+)$	0.831	1.294	6894		7212		6761
0 3 3 0 3	$1F(\frac{5}{2}^-)$	0.555	0.903	6518		6577	6313	6336
	$2F(\frac{5}{2}^-)$	0.553	1.064	6795		6863		6524
	$3F(\frac{5}{2}^-)$	0.619	1.646	7032		7114		
	$4F(\frac{5}{2}^-)$	1.110	0.960	7057		7339		
0 3 3 0 3	$1F(\frac{7}{2}^-)$	0.556	0.909	6523		6581		6331
	$2F(\frac{7}{2}^-)$	0.553	1.070	6801		6867		6521
	$3F(\frac{7}{2}^-)$	0.618	1.641	7034		7117		
	$4F(\frac{7}{2}^-)$	1.111	0.965	7060		7342		
0 4 4 0 4	$1G(\frac{7}{2}^+)$	0.554	1.048	6692		6760	6517	
	$2G(\frac{7}{2}^+)$	0.542	1.178	6970		7020		
	$3G(\frac{7}{2}^+)$	0.607	1.745	7167				
	$4G(\frac{7}{2}^+)$	1.119	1.095	7214				
0 4 4 0 4	$1G(\frac{9}{2}^+)$	0.555	1.052	6695		6762		
	$2G(\frac{9}{2}^+)$	0.544	1.189	6975		7032		
	$3G(\frac{9}{2}^+)$	0.605	1.737	7169				
	$4G(\frac{9}{2}^+)$	1.120	1.098	7217				

Table 5. Root mean square radii (fm) and the mass spectra (MeV) of the Ξ_b' family (Part I).

$l_\rho l_\lambda L s j$	$nL(J^P)$	$\langle r_\rho^2\rangle^{1/2}$	$\langle r_\lambda^2\rangle^{1/2}$	mass	exp.[28]	[52]	[56]	[59]
0 0 0 1 1	$1S(\frac{1}{2}^+)$	0.604	0.411	5943	5935.02(0.05)	5936	5970	5935
	$2S(\frac{1}{2}^+)$	0.741	0.697	6350		6329		6328
	$3S(\frac{1}{2}^+)$	0.998	0.559	6535		6687		6625
	$4S(\frac{1}{2}^+)$	0.804	1.063	6691		6978		6902
0 0 0 1 1	$1S(\frac{3}{2}^+)$	0.614	0.431	5971	5952.3(0.6) 5955.33(0.13)	5963	5980	5958
	$2S(\frac{3}{2}^+)$	0.735	0.716	6370		6342		6343
	$3S(\frac{3}{2}^+)$	1.017	0.566	6554		6695		6634
	$4S(\frac{3}{2}^+)$	0.793	1.087	6705		6984		6907
0 1 1 1 0	$1P(\frac{1}{2}^-)$	0.642	0.608	6238		6233	6188	
	$2P(\frac{1}{2}^-)$	0.709	0.866	6569		6611		
	$3P(\frac{1}{2}^-)$	1.074	0.705	6758		6915		
	$4P(\frac{1}{2}^-)$	0.772	1.296	6866		7174		
0 1 1 1 1	$1P(\frac{1}{2}^-)$	0.640	0.603	6232		6227		6138
	$2P(\frac{1}{2}^-)$	0.709	0.862	6564		6604		
	$3P(\frac{1}{2}^-)$	1.071	0.701	6754		6904		6521
	$4P(\frac{1}{2}^-)$	0.774	1.292	6863		7164		6679
0 1 1 1 1	$1P(\frac{3}{2}^-)$	0.643	0.610	6240		6234		
	$2P(\frac{3}{2}^-)$	0.709	0.868	6572		6605		
	$3P(\frac{3}{2}^-)$	1.076	0.707	6760		6905		
	$4P(\frac{3}{2}^-)$	0.771	1.297	6868		7163		
0 1 1 1 2	$1P(\frac{3}{2}^-)$	0.639	0.600	6229	6227.9(0.9)? 6226.8(1.6)?	6224	6190	6136
	$2P(\frac{3}{2}^-)$	0.709	0.859	6562		6598		6340
	$3P(\frac{3}{2}^-)$	1.069	0.700	6752		6900		6520
	$4P(\frac{3}{2}^-)$	0.774	1.291	6861		7159		6678
0 1 1 1 2	$1P(\frac{5}{2}^-)$	0.644	0.613	6243		6226	6201	6133
	$2P(\frac{5}{2}^-)$	0.708	0.871	6574		6596		6338
	$3P(\frac{5}{2}^-)$	1.077	0.708	6762		6897		6518
	$4P(\frac{5}{2}^-)$	0.770	1.299	6869		7156		6677
0 2 2 1 1	$1D(\frac{1}{2}^+)$	0.656	0.773	6460		6447		6247
	$2D(\frac{1}{2}^+)$	0.690	0.992	6757		6767		6440
	$3D(\frac{1}{2}^+)$	1.109	0.845	6941				6611
	$4D(\frac{1}{2}^+)$	0.754	1.464	7017				6763
0 2 2 1 1	$1D(\frac{3}{2}^+)$	0.658	0.780	6466		6459		
	$2D(\frac{3}{2}^+)$	0.690	0.998	6763		6775		
	$3D(\frac{3}{2}^+)$	1.111	0.850	6946				
	$4D(\frac{3}{2}^+)$	0.751	1.462	7020				

Table 6. Root mean square radii (fm) and the mass spectra (MeV) of the Ξ_b' family (Part II).

$l_\rho l_\lambda L s j$	$nL(J^P)$	$\langle r_\rho^2\rangle^{1/2}$	$\langle r_\lambda^2\rangle^{1/2}$	mass	[52]	[56]	[59]
0 2 2 1 2	$1D(\frac{3}{2}^+)$	0.656	0.773	6460	6431		6245
	$2D(\frac{3}{2}^+)$	0.690	0.992	6758	6751		6439
	$3D(\frac{3}{2}^+)$	1.109	0.845	6941			6610
	$4D(\frac{3}{2}^+)$	0.754	1.464	7017			6763
0 2 2 1 2	$1D(\frac{5}{2}^+)$	0.658	0.780	6466	6432	6393	
	$2D(\frac{5}{2}^+)$	0.690	0.999	6764	6751		
	$3D(\frac{5}{2}^+)$	1.112	0.851	6946			
	$4D(\frac{5}{2}^+)$	0.751	1.462	7021			
0 2 2 1 3	$1D(\frac{5}{2}^+)$	0.656	0.773	6460	6420		6241
	$2D(\frac{5}{2}^+)$	0.690	0.991	6757	6740		6437
	$3D(\frac{5}{2}^+)$	1.108	0.844	6941			6609
	$4D(\frac{5}{2}^+)$	0.754	1.464	7017			6762
0 2 2 1 3	$1D(\frac{7}{2}^+)$	0.658	0.781	6467	6414	6395	6237
	$2D(\frac{7}{2}^+)$	0.690	1.000	6765	6736		6434
	$3D(\frac{7}{2}^+)$	1.112	0.851	6946			6607
	$4D(\frac{7}{2}^+)$	0.751	1.461	7021			6761
0 3 3 1 2	$1F(\frac{3}{2}^-)$	0.663	0.931	6657	6675		6341
	$2F(\frac{3}{2}^-)$	0.678	1.121	6942			6527
	$3F(\frac{3}{2}^-)$	1.130	0.986	7110			
	$4F(\frac{3}{2}^-)$	0.734	1.580	7162			
0 3 3 1 2	$1F(\frac{5}{2}^-)$	0.664	0.936	6660	6686		
	$2F(\frac{5}{2}^-)$	0.680	1.130	6946			
	$3F(\frac{5}{2}^-)$	1.131	0.991	7114			
	$4F(\frac{5}{2}^-)$	0.732	1.573	7164			
0 3 3 1 3	$1F(\frac{5}{2}^-)$	0.663	0.931	6657	6640		6337
	$2F(\frac{5}{2}^-)$	0.678	1.121	6942			6524
	$3F(\frac{5}{2}^-)$	1.130	0.986	7110			
	$4F(\frac{5}{2}^-)$	0.734	1.580	7162			
0 3 3 1 3	$1F(\frac{7}{2}^-)$	0.664	0.936	6660	6641		
	$2F(\frac{7}{2}^-)$	0.680	1.131	6947			
	$3F(\frac{7}{2}^-)$	1.131	0.991	7114			
	$4F(\frac{7}{2}^-)$	0.731	1.572	7165			
0 3 3 1 4	$1F(\frac{7}{2}^-)$	0.663	0.931	6657	6619		6333
	$2F(\frac{7}{2}^-)$	0.678	1.121	6942			6524
	$3F(\frac{7}{2}^-)$	1.130	0.986	7110			
	$4F(\frac{7}{2}^-)$	0.734	1.580	7162			
0 3 3 1 4	$1F(\frac{9}{2}^-)$	0.664	0.937	6661	6610		6328
	$2F(\frac{9}{2}^-)$	0.680	1.132	6947			6519
	$3F(\frac{9}{2}^-)$	1.131	0.991	7114			
	$4F(\frac{9}{2}^-)$	0.731	1.572	7165			

Table 7. Fitted values for the slope and intercept of the Regge trajectories for the Ξ_c and Ξ'_c families.

Trajectory	$n=1$		$n=2$		$n=3$	
	α/GeV^2	β/GeV^2	α/GeV^2	β/GeV^2	α/GeV^2	β/GeV^2
$\bar{3}_F(NP)(NJ)$	1.493 ± 0.056	5.580 ± 0.160	1.433 ± 0.022	8.047 ± 0.063	1.507 ± 0.032	9.305 ± 0.091
$\bar{3}_F(UP)(UJ)$	1.456 ± 0.043	7.122 ± 0.098	1.446 ± 0.023	9.399 ± 0.052	1.501 ± 0.026	10.784 ± 0.059
$6_F(NP)(UJ)$	1.592 ± 0.058	6.098 ± 0.166	1.530 ± 0.033	8.611 ± 0.096	1.539 ± 0.031	9.574 ± 0.089
$6_F(UP)(UJ)$	1.487 ± 0.033	7.959 ± 0.076	1.473 ± 0.026	10.292 ± 0.059	1.482 ± 0.018	11.260 ± 0.041
$6_F(NP)(UJ)$	1.433 ± 0.026	9.545 ± 0.044	1.433 ± 0.026	11.837 ± 0.045	1.453 ± 0.015	12.795 ± 0.026
$6_F(UP)(NJ)$	1.507 ± 0.040	4.933 ± 0.153	1.459 ± 0.022	7.451 ± 0.082	1.474 ± 0.019	8.371 ± 0.071
$6_F(NP)(NJ)$	1.455 ± 0.031	6.618 ± 0.098	1.437 ± 0.025	8.980 ± 0.079	1.454 ± 0.018	9.911 ± 0.058
$6_F(UP)(NJ)$	1.463 ± 0.034	8.041 ± 0.078	1.444 ± 0.025	10.383 ± 0.057	1.460 ± 0.019	11.336 ± 0.043

Table 8. Fitted values for the slope and intercept of the Regge trajectories for the Ξ_b and Ξ'_b families.

Trajectory	$n=1$		$n=2$		$n=3$	
	α/GeV^2	β/GeV^2	α/GeV^2	β/GeV^2	α/GeV^2	β/GeV^2
$\bar{3}_F(NP)(NJ)$	2.760 ± 0.134	32.756 ± 0.386	2.470 ± 0.027	37.595 ± 0.077	2.341 ± 0.122	41.187 ± 0.350
$\bar{3}_F(UP)(UJ)$	2.582 ± 0.099	35.891 ± 0.226	2.449 ± 0.014	40.029 ± 0.033	2.190 ± 0.114	43.86 ± 0.262
$6_F(NP)(UJ)$	2.820 ± 0.129	34.316 ± 0.371	2.592 ± 0.032	39.116 ± 0.092	2.518 ± 0.076	41.681 ± 0.219
$6_F(UP)(UJ)$	2.605 ± 0.087	37.677 ± 0.199	2.529 ± 0.014	41.849 ± 0.033	2.388 ± 0.051	44.509 ± 0.116
$6_F(NP)(UJ)$	2.465 ± 0.068	40.538 ± 0.117	2.512 ± 0.013	44.409 ± 0.022	2.309 ± 0.038	47.045 ± 0.065
$6_F(UP)(NJ)$	2.747 ± 0.113	31.888 ± 0.428	2.536 ± 0.019	36.834 ± 0.072	2.462 ± 0.062	39.454 ± 0.235
$6_F(NP)(NJ)$	2.580 ± 0.085	35.207 ± 0.273	2.510 ± 0.016	39.450 ± 0.050	2.374 ± 0.053	42.222 ± 0.170
$6_F(UP)(NJ)$	2.588 ± 0.089	37.766 ± 0.205	2.522 ± 0.018	41.921 ± 0.041	2.382 ± 0.057	44.573 ± 0.131

References

[1] P. Avery *et al.* (CLEO Collaboration), Phys. Rev. Lett. **75**, 4364-4368 (1995), arXiv:hep-ex/9508010

[2] R. Mizuk *et al.* (Belle Collaboration), Phys. Rev. Lett. **94**, 122002 (2005), arXiv:hep-ex/0412069

[3] B. Aubert *et al.* (BaBar Collaboration), arXiv: hep-ex/0607042

[4] B. Aubert *et al.* (BABAR Collaboration), Phys. Rev. D **77**, 012002 (2008), arXiv:0710.5763[hep-ex]

[5] B. Aubert *et al.* (BaBar Collaboration), Phys. Rev. Lett. **97**, 232001 (2006), arXiv:hep-ex/0608055

[6] B. Aubert *et al.* (BaBar Collaboration), Phys. Rev. Lett. **98**, 012001 (2007), arXiv:hep-ex/0603052

[7] K. Abe *et al.* (Belle Collaboration), Phys. Rev. Lett. **98**, 262001 (2007), arXiv:hep-ex/0608043

[8] B. Aubert *et al.* (BaBar Collaboration], Phys. Rev. D **77**, 031101 (2008)

[9] T. Lesiak *et al.* (Belle Collaboration), Phys. Lett. B **665**, 9 (2008), arXiv:0802.3968[hep-ex]

[10] Y. Kato *et al.* (Belle Collaboration), Phys. Rev. D **89**, 052003 (2014), arXiv:1312.1026[hep-ex]

[11] E. Solovieva *et al.*, Phys. Lett. B **672**, 1 (2009), arXiv:0808.3677[hep-ex]

[12] Y. B. Li *et al.* (Belle Collaboration), Eur. Phys. J. C **78**, 928 (2018), arXiv:1806.09182[hep-ex]

[13] R. Aaij *et al.* (LHCb collaboration), Phys. Rev. Lett. **124**, 222001 (2020), arXiv:2003.13649[hep-ex]

[14] T. J. Moon *et al.* (Belle Collaboration), Phys. Rev. D **103**, 111101 (2021), arXiv:2007.14700[hep-ex]

[15] Y. Kato *et al.* (Belle Collaboration), Phys. Rev. D **94**, 032002 (2016), arXiv:1605.09103[hep-ex]

[16] P. Abreu *et al.* (DELPHI Collaboration), Z. Phys. C **68**, 541 (1995)

[17] V. Abazov *et al.* (D0 Collaboration), Phys. Rev. Lett. **99**, 052001 (2007), arXiv:0706.1690[hep-ex]

[18] T. Aaltonen *et al.* (CDF Collaboration), Phys. Rev. Lett. **99**, 052002 (2007), arXiv:0707.0589[hep-ex]

[19] T. Aaltonen (CDF Collaboration), Phys. Rev. Lett. **107**, 102001 (2011), arXiv:1107.4015[hep-ex]

[20] CMS Collaboration, Phys. Rev. Lett **108**, 252002 (2012), arXiv:1204.5955[hep-ex]

[21] R. Aaij *et al.* (LHCb Collaboration), Phys. Rev. Lett. **114**, 062004 (2015)

[22] R. Aaij *et al.* (LHCb Collaboration), J. High Energy Phys. **05**, 161 (2016)

[23] R. Aaij *et al.* (LHCb Collaboration), Phys. Rev. Lett. **121**, 072002 (2018)

[24] A. M. Sirunyan *et al.* (CMS Collaboration), Phys. Rev. Lett. **126**, 252003 (2021)

[25] R. Aaij *et al.*, Phys. Rev. Lett. **128**, 162001 (2022), arXiv:2110.04497[hep-ex]
[26] R. Aaij *et al.* (LHCb Collaboration), Phys. Rev. Lett. **122**, 012001 (2019), arXiv:1809.07752
[27] R. Aaij *et al.* (LHCb Collaboration), Phys. Rev. Lett. **123**, 152001 (2019)
[28] P. A. Zyla et al. (Particle Data Group), Prog. Theor. Exp. Phys. 083C01 (2020); R. L. Workman et al. (Particle Data Group), Prog. Theor. Exp. Phys. 2022, 083C01 (2022) and 2022 update online
[29] R.Chistov *et al.* (Belle Collaboration), Phys. Rev. Lett. **97**, 162001 (2006)
[30] L. H. Liu, L. Y. Xiao, and X. H. Zhong, Phys. Rev. D **86**, 034024 (2012), arXiv:1205.2943[hep-ph]
[31] D. D. Ye, Z. Zhao and A. Zhang, Phys. Rev. D **96**, 114009 (2017), arXiv:1709.00689[hep-ph]
[32] Z. Zhao, D. D. Ye and A. Zhang, Phys. Rev. D **94**, 114020 (2016)
[33] Y. X. Yao, K. L. Wang and X. H. Zhong, Phys. Rev. D **98**, 076015 (2018), arXiv:1803.00364
[34] D. D. Ye, Z. Zhao and A. Zhang, Phys. Rev. D **96**, 114003 (2017), arXiv:1710.10165[hep-ph]
[35] Z. G. Wang, Nucl. Phys. B **926**, 467 (2018), arXiv:1705.07745[hep-ph]
[36] B. Roelof, G. T. Hugo, G. Alessandro *et al.*, arXiv: 2010.12437[hep-ph]
[37] K. L. Wang, Y. X. Yao, X. H. Zhong *et al.*, Phys. Rev. D **96**, 116016 (2017), arXiv:hep-ph/1709.04268
[38] B. Chen, X. Liu and A. Zhang, Phys. Rev. D **95**, 074022 (2017)
[39] Z. G. Wang and H. J. Wang, Chin. Phys. C **45**, 013109 (2021), arXiv:2006.16776[hep-ph]
[40] J. Nieves, R. Pavao and L. Tolos, Eur. Phys. J. C **80**, 22 (2020), arXiv:1911.06089[hep-ph]
[41] Z. Zhao, Phys. Rev. D **102**, 096021 (2020), arXiv:2008.00630[hep-ph]
[42] B. Chen, K. W. Wei and A. Zhang, Eur. Phys. J. A **51**, 82 (2015), arXiv:1406.6561[hep-ph]
[43] K. L. Wang, Q. F. Lü, and X. H. Zhong, Phys. Rev. D **99**, 014011 (2019)
[44] Y. Huang, C. J. Xiao, L. S. Geng *et al.*, Phys. Rev. D **99**, 014008 (2019)
[45] B. Chen, K. W. Wei, X. Liu *et al.*, Phys. Rev. D **98**, 031502 (2018), arXiv:1805.10826[hep-ph]
[46] H. J. Wang, Z. Y. Di and Z. G. Wang, Int. J. Theor. Phys. **59**(10), 3124-3133 (2020)
[47] K. Azizi, Y. Sarac, and H. Sundu, J. of High Energy Phys. **2021**, 244 (2021), arXiv:2012.01086[hep-ph]
[48] G. L. Yu, Z. G. Wang and X. W. Wang, arXiv: 2109.02217[hep-ph]
[49] H. M. Yang, H. X. Chen, E. L. Cui *et al.*, arXiv: 2205.07224[hep-ph]
[50] W. J. Wang, Y. H. Zhou, L. Y. Xiao *et al.*, Phys. Rev. D **105**, 074008 (2022), arXiv:2202.05426[hep-ph]
[51] D. Ebert, R. N. Faustov and V. O. Galkin, Phys. Lett. B **659**, 612 (2008), arXiv:0705.2957v2
[52] D. Ebert, R. N. Faustov and V. O. Galkin, Phys. Rev. D **84**, 014025 (2011)
[53] R. N. Faustov and V. O. Galkin, Phys. Rev. D **105**, 014013 (2022), arXiv:hep-ph/2111.07702v1
[54] H. Mutuk, Eur. Phys. J. Plus **137**, 10 (2022), arXiv:hep-ph/2112.06205v1
[55] S. Capstick and N.Isgur, Phys. Rev. D **34**, 2809 (1986)
[56] W. Roberts, M. Pervin, International Journal of Modern Physics A **23**(19), 2817-2860 (2008)
[57] B. Chen, K. W. Wei, X. Liu *et al.*, Eur. Phys. J. C **77**(3), 154 (2017), arXiv:1609.07967[hep-ph]
[58] K. Gandhi, A. K. Rai, Eur. Phys. J. Plus **135**(2), 213 (2020), arXiv:1911.11039[hep-ph]
[59] A. Kakadiya, Z. Shah, and A. K. Rai, International Journal of Modern Physics A **37**, 2250053 (2022), arXiv:2202.12048[hep-ph]
[60] T. Yoshida, E. Hiyama, A. Hosaka *et al.*, Phys. Rev. D **92**, 114029 (2015), arXiv:hep-ph/1510.01067
[61] G. Yang, J. Ping, and J. Segovia, Few Body Syst. **59**, 113 (2018), arXiv:1709.09315[hep-ph]
[62] G. Yang, J. Ping, P. G. Ortega *et al.*, Chin. Phys. C **44**, 023102 (2020), arXiv:1904.10166[hep-ph]
[63] J. Segovia, D. R. Entem, F. Fernandez *et al.*, Int. J. Mod. Phys. E **22**, 1330026 (2013), arXiv:1309.6926
[64] M. Q. Huang, Y. B. Dai, and C. S. Huang, Phys. Rev. D 52, 3986 (1995), [Erratum: Phys. Rev. D **55**, 7317(E) (1997)
[65] M. C. Banuls, A. Pich and I. Scimemi, Phys. Rev. D **61**, 094009 (2000)
[66] H. Y. Cheng and C. K. Chua, Phys. Rev. D **75**, 014006 (2007)
[67] N. Jiang, X. L. Chen and S. L. Zhu, Phys. Rev. D **92**, 054017 (2015)
[68] H. Y. Cheng and C. K. Chua, Phys. Rev. D **92**, 074014 (2015)
[69] X. H. Guo, K. W. Wei and X. H. Wu, Phys. Rev. D **77**, 036003 (2008)
[70] G. L. Yu, Z. G. Wang and Z. Y. Li, Chin. Phys. C **39**(6), 063101 (2015), arXiv:hep-ph/1402.5955
[71] H. Z. He, W. Liang and Q. F. Lü, Phys. Rev. D **105**, 014010 (2022), arXiv:hep-ph/2106.11045v2
[72] C. Chen, X. L. Chen, X. Liu *et al.*, Phys. Rev. D **75**, 094017 (2007)
[73] P. Yang, J. J. Guo and A. Zhang, Phys. Rev. D **99**, 034018 (2019), arXiv:1810.06947[hep-ph]
[74] J. J. Guo, P. Yang, and A. Zhang, Phys. Rev. D **100**, 014001 (2019), arXiv:1902.07488[hep-ph]
[75] W. Liang, Q. F. Lü and X. H. Zhong, Phys. Rev. D **100**, 054013 (2019)
[76] Q. F. Lü and X. H. Zhong, Phys. Rev. D **101**, 014017 (2020)
[77] H. Z. He, W. Liang, Q. F. Lü *et al.*, Sci. China Phys. Mech. Astron. **64**, 261012 (2021)
[78] M. Padmanath, R. G. Edwards, N. Mathur *et al.*, arXiv: 1311.4806
[79] H. Bahtiyar, K. U. Can, G. Erkol *et al.*, Phys. Lett. B **747**, 281 (2015)
[80] P. Perez-Rubio, S. Collins and G. S. Bali, Phys. Rev. D **92**, 034504 (2015)
[81] H. Bahtiyar, K. U. Can, G. Erkol *et al.*, Phys. Lett. B **772**, 121 (2017)
[82] C. K. Chow, Phys. Rev. D **54**, 3374 (1996)
[83] S. L. Zhu and Y. B. Dai, Phys. Rev. D **59**, 114015 (1999)
[84] S. S. Agaev, K. Azizi and H. Sundu, Phys. Rev. D **96**, 094011 (2017)
[85] H. X. Chen, Q. Mao, W. Chen *et al.*, Phys. Rev. D **95**, 094008 (2017)
[86] Z. G. Wang, Phys. Rev. D **81**, 036002 (2010)
[87] Z. G. Wang, Eur. Phys. J. A **44**, 105 (2010)
[88] T. M. Aliev, K. Azizi and H. Sundu, Eur. Phys. J. C **75**, 14

(2015)
[89] T. M. Aliev, K. Azizi and A. Ozpineci, Phys. Rev. D **79**, 056005 (2009)
[90] T. M. Aliev, T. Barakat and M. Savc, Phys. Rev. D **93**, 056007 (2016)
[91] T. M. Aliev, K. Azizi and M. Savci, Phys. Lett. B **696**, 220 (2011)
[92] T. M. Aliev, K. Azizi, Y. Sarac *et al*., Phys. Rev. D **99**, 094003 (2019)
[93] S. L. Zhu, Phys. Rev. D **61**, 114019 (2000)
[94] Z. G. Wang, Eur. Phys. J. A **47**, 81 (2011)
[95] Q. Mao, H. X. Chen, W. Chen *et al*., Phys. Rev. D **92**, 114007 (2015), arXiv:1510.05267[hep-ph]
[96] H. X. Chen, Q. Mao, A. Hosaka *et al*., Phys. Rev. D **94**, 114016 (2016)
[97] Q. Mao, H. X. Chen, A. Hosaka *et al*., Phys. Rev. D **96**, 074021 (2017)
[98] T. M. Aliev, K. Azizi, Y. Sarac *et al*., Phys. Rev. D **98**, 094014 (2018)
[99] E. L. Cui, H. M. Yang, H. X. Chen *et al*., Phys.Rev. D **99**, 094021 (2019)
[100] K. Azizi, Y. Sarac and H. Sundu, Phys. Rev. D **101**, 074026 (2020)
[101] K. Azizi, Y. Sarac and H. Sundu, Phys. Rev. D **102**, 034007 (2020)
[102] Z. G. Wang, Eur. Phys. J. C **75**(8), 359 (2015)
[103] S. Godfrey and N. Isgur, Phys. Rev. D **32**, 189 (1985)
[104] E. Hiyama, Y. Kino and M. Kamimura, Prog. Part. Nucl. Phys. **51**, 223 (2003)
[105] Q. F. Lü, D. Y. Chen and Y. B. Dong, Phys. Rev. D **102**, 034012 (2020)
[106] Q. F. Lü, D. Y. Chen and Y. B. Dong, Eur. Phys. J. C **80**, 871 (2020)
[107] Q. F. Lü, D. Y. Chen and Y. B. Dong, Phys. Rev. D **102**, 074021 (2020)
[108] E. Hiyama, A. Hosaka, M. Oka *et al*., Phys. Rev. C **98**, 045208 (2018), arXiv:1803.11369v1[nucl-th]
[109] H. X. Chen, W. Chen, X. Liu *et al*., Physics Reports **639**, 1-121 (2016), arXiv:1601.02092[hep-ph]
[110] F. K. Guo, C. Hanhart, U. G. Meißner *et al*., Rev. Mod. Phys. **90**, 015004 (2018), arXiv:1705.00141[hep-ph]
[111] R. Aaij *et al*., Phys. Rev. Lett. **122**, 222001 (2019), arXiv:1904.03947[hep-ex]
[112] X. K. Dong, F. K. Guo, B. S. Zou, Commun. Theor. Phys. **73**, 125201 (2021), arXiv:2108.02673[hep-ph]
[113] T. Ji, X. K. Dong, F. K. Guo *et al*., Phys. Rev. Lett. **129**, 102002 (2022), arXiv:2205.10994[hep-ph]
[114] C. Q. Pang, J. Z. Wang, X. Liu *et al*., Eur. Phys. J. C **77**, 861 (2017)
[115] G. L. Yu, Z. Y. Li, Z. G. Wang *et al*., Nucl. Phys. B **990**, 116183 (2023), arXiv:2206.08128[hep-ph]
[116] H. Georgi, Physics Letters B **240**, 447-450 (1990)
[117] B. Chen, S. Q. Luo, X. Liu *et al*., Phys. Rev. D **100**, 094032 (2019), arXiv:1910.03318
[118] Y. W. Pan, T. W. Wu, M. Z. Liu *et al*., Phys. Rev. D **105**, 114048 (2022), arXiv:2204.02295
[119] H. Garcilazo, J. Vijande and A. Valcarce, J. phys. G **34**, 961 (2007)
[120] S. Migura, D. Merten, B. Metsch *et al*., Eur. Phys. J. A **28**, 41 (2006)
[121] A. Martin, Z. Phys. C **32**, 359 (1986)
[122] T. Regge, Nuovo Cim. **14**, 951 (1959)
[123] T. Regge, Nuovo Cim. **18**, 947-956 (1960)
[124] G. F. Chew and S. C. Frautschi, Phys. Rev. Lett. **7**, 394-397 (1961)
[125] G. F. Chew and S. C. Frautschi, Phys. Rev. Lett. **8**, 41-44 (1962)
[126] M. Baker and R. Steinke, Phys. Rev. D **65**, 094042 (2002)
[127] P. D. B. Collins, An Introduction to Regge Theory and High Energy Physics (Cambridge, Cambridge University Press, England, 1977)